



iJRASET

International Journal For Research in
Applied Science and Engineering Technology



INTERNATIONAL JOURNAL FOR RESEARCH

IN APPLIED SCIENCE & ENGINEERING TECHNOLOGY

Volume: 11 Issue: VIII Month of publication: Aug 2023

DOI: <https://doi.org/10.22214/ijraset.2023.55280>

www.ijraset.com

Call:  08813907089

E-mail ID: ijraset@gmail.com

Spectral and Up conversion Properties of Ho^{3+} ions doped Zinc Lithium Lead Soda lime Cadmium Phosphate Glasses

Dr. S. L. Meena

Ceramic Laboratory, Department of physics, Jai Narain Vyas University, Jodhpur 342001(Raj) India

Abstract: Glasses samples containing Ho^{3+} in zinc lithium lead sodalime cadmium phosphate $(35-x)\text{P}_2\text{O}_5:10\text{ZnO}:10\text{Li}_2\text{O}:10\text{PbO}:10\text{CaO}:10\text{Na}_2\text{O}:15\text{CdO}:x\text{Ho}_2\text{O}_3$ (where $x=1, 1.5, 2$ mol %) have been prepared by melt-quenching method. The amorphous nature of the prepared glass samples was confirmed by X-ray diffraction. Optical absorption, Excitation and fluorescence spectra were recorded at room temperature for all glass samples. Judd-Ofelt intensity parameters Ω_λ ($\lambda=2, 4$ and 6) are evaluated from the intensities of various absorption bands of optical absorption spectra. Using these intensity parameters various radiative properties like spontaneous emission probability (A), branching ratio (β), radiative life time (τ_R) and stimulated emission cross-section (σ_p) of various emission lines have been evaluated.

Keywords: ZLLSLCP Glasses, Optical Properties, Judd-Ofelt Theory, Upconversion Properties.

I. INTRODUCTION

Rare earth doped glasses have attracted a great deal of attention because of their applications in thermal imaging, fiber amplifiers, laser fusion, optical fibers, photovoltaic solar cells, optical communications, up-conversion lasers and optical data storage [1–5]. Among different glasses, phosphate glasses have unique properties. They have high transparency, high thermal stability, optical stability and low phonon energy. Phosphate glasses possess excellent physicochemical properties, optical properties, lower phonon energy, better color rendering index (CRI), and low melting temperature [6–10]. The low nonlinear dispersion of the highly rare earth doped phosphate glasses enables there in high power applications. The low glass melting temperature makes the phosphate glasses suitable candidates for photonic applications. Phosphate glasses also exhibit high rare earth solubility [11,12]. Addition of network modifier (NMF) Li_2O to the phosphate glasses improves both electrical and mechanical properties of such glasses [13]. ZnO is also added due to its specific chemical and microstructure properties. Addition of PbO to the phosphate glass improves the chemical stability of glass network. Ho^{3+} ions the most studied among the rare earth ions and the up conversion process of this ion in various kinds of host materials has been investigated [14–18].

The present work reports on the preparation and characterization of rare earth doped heavy metal oxide (HMO) glass systems for lasing materials. I have studied on the Optical absorption, Excitation and fluorescence spectra of Ho^{3+} doped zinc lithium lead sodalime cadmium phosphate glasses. The intensities of the transitions for the rare earth ions have been estimated successfully using the Judd-Ofelt theory. The laser parameters such as radiative probabilities (A), branching ratio (β), radiative life time (τ_R) and stimulated emission cross section (σ_p) are evaluated using J.O. intensity parameters (Ω_λ , $\lambda=2, 4$ and 6).

II. EXPERIMENTAL TECHNIQUES

A. Preparation of Glasses

The following Ho^{3+} doped phosphate glass samples $(35-x)\text{P}_2\text{O}_5:10\text{ZnO}:10\text{Li}_2\text{O}:10\text{PbO}:10\text{CaO}:10\text{Na}_2\text{O}:15\text{CdO}:x\text{Ho}_2\text{O}_3$ (where $x=1, 1.5$ and 2 mol%) have been prepared by melt-quenching method. Analytical reagent grade chemical used in the present study consist of P_2O_5 , ZnO , Li_2O , PbO , CaO , Na_2O , CdO and Ho_2O_3 .

They were thoroughly mixed by using an agate pestle mortar. then melted at 1072°C by an electrical muffle furnace for 2h., After complete melting, the melts were quickly poured in to a preheated stainless steel mould and annealed at temperature of 250°C for 2h to remove thermal strains and stresses. Every time fine powder of cerium oxide was used for polishing the samples. The glass samples so prepared were of good optical quality and were transparent. The chemical compositions of the glasses with the name of samples are summarized in Table 1.

Table 1.

Chemical composition of the glasses

| Sample | Glass composition (mol %) |
|----------------|---------------------------------------------------------------------------------------------------------------------------------------|
| ZLLSLCP(UD) | 35P ₂ O ₅ :10ZnO:10Li ₂ O:10PbO:10CaO:10Na ₂ O:15CdO |
| ZLLSLCP (HO1) | 34P ₂ O ₅ :10ZnO:10Li ₂ O:10PbO:10CaO:10Na ₂ O:15CdO:1 Ho ₂ O ₃ |
| ZLLSLCP(HO1.5) | 33.5P ₂ O ₅ :10ZnO:10Li ₂ O:10PbO:10CaO:10Na ₂ O:15CdO:1.5 Ho ₂ O ₃ |
| ZLLSLCP(HO2) | 33P ₂ O ₅ :10ZnO:10Li ₂ O:10PbO:10CaO:10Na ₂ O:15CdO:2 Ho ₂ O ₃ |
| ZLLSLCP (UD) | -Represents undoped Zinc Lithium Lead Sodalime Cadmium Phosphate glass specimens |
| ZLLSLCP (HO) | -Represents Ho ³⁺ doped Zinc Lithium Lead Sodalime Cadmium Phosphate glass specimens |

III. THEORY

A. Oscillator Strength

The intensity of spectral lines are expressed in terms of oscillator strengths using the relation [19].

$$f_{\text{expt.}} = 4.318 \times 10^{-9} \int \epsilon(\nu) d\nu \quad (1)$$

where, $\epsilon(\nu)$ is molar absorption coefficient at a given energy ν (cm⁻¹), to be evaluated from Beer–Lambert law.

Under Gaussian Approximation, using Beer–Lambert law, the observed oscillator strengths of the absorption bands have been experimentally calculated [20], using the modified relation:

$$P_m = 4.6 \times 10^{-9} \times \frac{1}{cl} \log \frac{I_0}{I} \times \Delta\nu_{1/2} \quad (2)$$

where c is the molar concentration of the absorbing ion per unit volume, l is the optical path length, $\log I_0/I$ is optical density and $\Delta\nu_{1/2}$ is half band width.

B. Judd-Ofelt Intensity Parameters

According to Judd [21] and Ofelt [22] theory, independently derived expression for the oscillator strength of the induced forced electric dipole transitions between an initial J manifold $|4f^N(S, L) J\rangle$ level and the terminal J' manifold $|4f^N(S', L') J'\rangle$ is given by:

$$\frac{8\pi^2 m c \bar{\nu}}{3h(2J+1)n} \left[\frac{(n^2+2)^2}{9} \right] \times S(J, J') \quad \text{Where,} \quad (3)$$

the line strength $S(J, J')$ is given by the equation

$$S(J, J') = e^2 \sum_{\lambda=2,4,6} \Omega_{\lambda} \langle 4f^N(S, L) J \| U^{(\lambda)} \| 4f^N(S', L') J' \rangle^2 \quad (4)$$

In the above equation m is the mass of an electron, c is the velocity of light, $\bar{\nu}$ is the wave number of the transition, h is Planck's constant, n is the refractive index, J and J' are the total angular momentum of the initial and final level respectively, Ω_{λ} ($\lambda=2,4$ and 6) are known as Judd-Ofelt intensity.

C. Radiative Properties

The Ω_{λ} parameters obtained using the absorption spectral results have been used to predict radiative properties such as spontaneous emission probability (A) and radiative life time (τ_R), and laser parameters like fluorescence branching ratio (β_R) and stimulated emission cross section (σ_p).

The spontaneous emission probability from initial manifold $|4f^N(S', L') J'\rangle$ to a final manifold $|4f^N(S, L) J\rangle$ is given by:

$$A[(S', L') J'; (S, L) J] = \frac{64\pi^2 \bar{\nu}^3}{3h(2J'+1)} \left[\frac{n(n^2+2)^2}{9} \right] \times S(J', J) \quad (5)$$

Where, $S(J', J) = e^2 [\Omega_2 \| U^{(2)} \|^2 + \Omega_4 \| U^{(4)} \|^2 + \Omega_6 \| U^{(6)} \|^2]$

The fluorescence branching ratio for the transitions originating from a specific initial manifold $|4f^N(S', L') J' \rangle$ to a final many fold $|4f^N(S, L) J \rangle$ is given by

$$\beta[(S', L') J'; (S, L) J] = \frac{A[(S', L') J' \rightarrow (S, L) J]}{\sum_{S, L, J} A[(S', L') J' \rightarrow (S, L) J]} \quad (6)$$

where, the sum is over all terminal manifolds.

The radiative life time is given by

$$\tau_{rad} = \frac{1}{\sum_{S, L, J} A[(S', L') J'; (S, L) J]} = A_{Total}^{-1} \quad (7)$$

where, the sum is over all possible terminal manifolds. The stimulated emission cross-section for a transition from an initial manifold $|4f^N(S', L') J' \rangle$ to a final manifold $|4f^N(S, L) J \rangle$ is expressed as

$$\sigma_p(\lambda_p) = \left[\frac{\lambda_p^4}{8\pi c n^2 \Delta\lambda_{eff}} \right] \times A[(S', L') J'; (\bar{S}, \bar{L}) \bar{J}] \quad (8)$$

where, λ_p the peak fluorescence wavelength of the emission band and $\Delta\lambda_{eff}$ is the effective fluorescence line width.

D. Nephelauxetic Ratio (β') and Bonding Parameter ($b^{1/2}$)

The nature of the R-O bond is known by the Nephelauxetic Ratio (β') and Bonding Parameters ($b^{1/2}$), which are computed by using following formulae [23, 24]. The Nephelauxetic Ratio is given by

$$\beta' = \frac{\nu_g}{\nu_a} \quad (9)$$

where, ν_a and ν_g refer to the energies of the corresponding transition in the glass and free ion, respectively. The value of bonding parameter ($b^{1/2}$) is given by

$$b^{1/2} = \left[\frac{1 - \beta'}{2} \right]^{1/2} \quad (10)$$

IV. RESULT AND DISCUSSION

A. XRD Measurement

Figure 1 presents the XRD pattern of the sample contain – P_2O_5 which is show no sharp Bragg's peak, but only a broad diffuse hump around low angle region. This is the clear indication of amorphous nature within the resolution limit of XRD instrument.

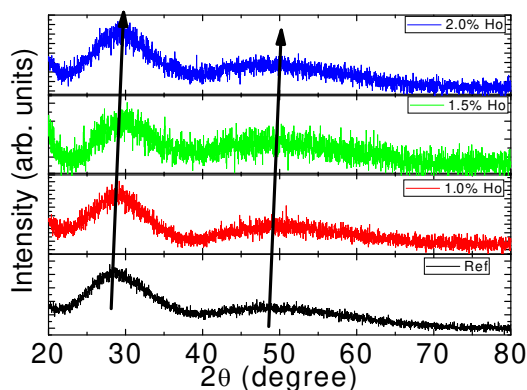


Fig. 1 X-ray diffraction pattern of ZLLSLCP (HO) Glasses.

B. Up conversion Emission Mechanism

Up-conversion emission mechanism for the zinc lithium lead sodalime cadmium phosphate glasses are schematically depicted as fig.2

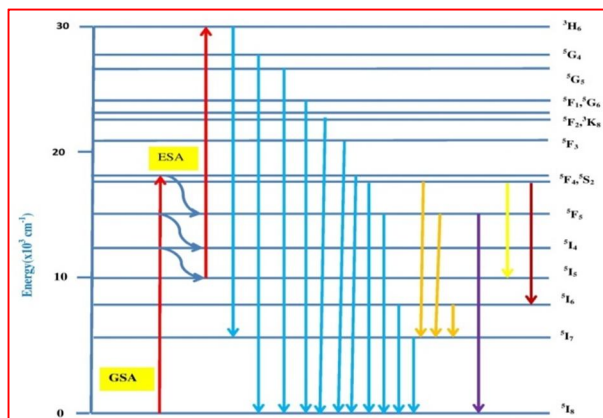


Fig. (2) Upconversion emission Mechanism.

C. Absorption Spectrum

The absorption spectra of Ho³⁺doped ZLLSLCP glass specimens have been presented in Figure 3 in terms of optical density versus wavelength. Twelve absorption bands have been observed from the ground state ⁵I₈ to excited states ⁵I₅, ⁵I₄, ⁵F₅, ⁵F₄, ⁵F₃, ³K₈, ⁵G₆, (⁵G, ³G)₅, ⁵G₄, ⁵G₂, ⁵G₃, and ³F₄ for Ho³⁺ doped ZLLSLCP glasses.

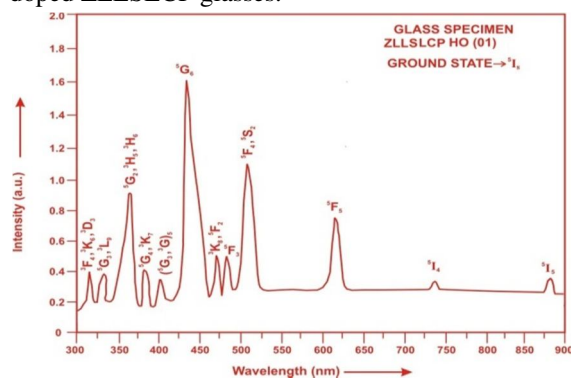


Fig. (3) Absorption spectrum of ZLLSLCP HO (01) glass.

The experimental and calculated oscillator strength for Ho³⁺ ions in ZLLSLCP glasses are given in **Table 3**.

Table 3: Measured and calculated oscillator strength ($P_m \times 10^{+6}$) of Ho³⁺ions in ZLLSLCP glasses.

| Energy level from ⁵ I ₈ | Glass ZLLSLCP (HO01) | | Glass ZLLSLCP (HO1.5) | | Glass ZLLSLCP (HO02) | |
|--------------------------------------------------|-------------------------|-------------------|--------------------------|-------------------|-------------------------|-------------------|
| | P _{exp.} | P _{cal.} | P _{exp.} | P _{cal.} | P _{exp.} | P _{cal.} |
| ⁵ I ₅ | 0.40 | 0.24 | 0.43 | 0.24 | 0.39 | 0.24 |
| ⁵ I ₄ | 0.05 | 0.02 | 0.04 | 0.02 | 0.03 | 0.02 |
| ⁵ F ₅ | 3.68 | 2.81 | 3.65 | 2.79 | 3.61 | 2.76 |
| ⁵ F ₄ | 4.72 | 4.37 | 4.69 | 4.33 | 4.65 | 4.29 |
| ⁵ F ₃ | 1.55 | 2.43 | 1.52 | 2.41 | 1.48 | 2.39 |
| ³ K ₈ | 1.48 | 1.98 | 1.45 | 1.96 | 1.41 | 1.93 |
| ⁵ G ₆ | 24.86 | 26.84 | 23.72 | 23.72 | 24.65 | 22.67 |
| (⁵ G, ³ G) ₅ | 3.82 | 1.70 | 3.78 | 1.68 | 3.75 | 1.66 |
| ⁵ G ₄ | 0.07 | 0.61 | 0.06 | 0.60 | 0.05 | 0.59 |
| ⁵ G ₂ | 5.86 | 5.31 | 5.83 | 5.11 | 5.79 | 4.91 |
| ⁵ G ₃ | 1.53 | 1.39 | 1.50 | 1.37 | 1.46 | 1.34 |
| ⁵ F ₄ | 1.44 | 4.18 | 1.41 | 4.13 | 1.38 | 4.09 |
| r.m.s. deviation | ±1.1018 | | ±1.1030 | | ±1.1077 | |

Computed values of F_2 , Lande' parameter (ξ_{4f}), Nephelauxetic ratio (β') and bonding parameter ($b^{1/2}$) for Ho^{3+} ions in ZLLSLCP glass specimen are given in Table 3.

Table 3: F_2 , ξ_{4f} , β' and $b^{1/2}$ parameters for Holmium doped glass specimen.

| Glass Specimen | F_2 | ξ_{4f} | β' | $b^{1/2}$ |
|------------------|--------|------------|----------|-----------|
| Ho^{3+} | 358.82 | 1258.16 | 0.9337 | 0.1821 |

In the Zinc Lithium Lead Sodalime Cadmium Phosphate glasses (ZLLSLCP) Ω_2 , Ω_4 and Ω_6 parameters decrease with the increase of x from 1 to 2 mol%. The order of magnitude of Judd-Ofelt intensity parameters is $\Omega_2 > \Omega_6 > \Omega_4$ for all the glass specimens. The spectroscopic quality factor (Ω_4 / Ω_6) related with the rigidity of the glass system has been found to lie between 0.603 and 0.608 in the present glasses.

The values of Judd-Ofelt intensity parameters are given in Table 4.

Table 4: Judd-Ofelt intensity parameters for Ho^{3+} doped ZLLSLCP glass specimens.

| Glass Specimen | $\Omega_2(\text{pm}^2)$ | $\Omega_4(\text{pm}^2)$ | $\Omega_6(\text{pm}^2)$ | Ω_4 / Ω_6 |
|-----------------|-------------------------|-------------------------|-------------------------|-----------------------|
| ZLLSLCP (HO01) | 5.817 | 1.302 | 2.140 | 0.6084 |
| ZLLSLCP (HO1.5) | 5.506 | 1.282 | 2.125 | 0.6033 |
| ZLLSLCP (HO02) | 5.212 | 1.269 | 2.104 | 0.6031 |

D. Excitation Spectrum

The Excitation spectrum of ZLLSLCP (HO 01) glass has been presented in Figure 4 in terms of Excitation Intensity versus wavelength. The excitation spectrum was recorded in the spectral region 325–525 nm fluorescence at 545nm having different excitation band centered at 349,419, 452, 473and 486 nm are attributed to the 5G_3 , ($^5G, ^3G$)₅, 5G_6 , 3K_8 and 5F_3 transitions, respectively. The highest absorption level is 5G_6 and is at 452nm. So this is to be chosen for excitation wavelength.

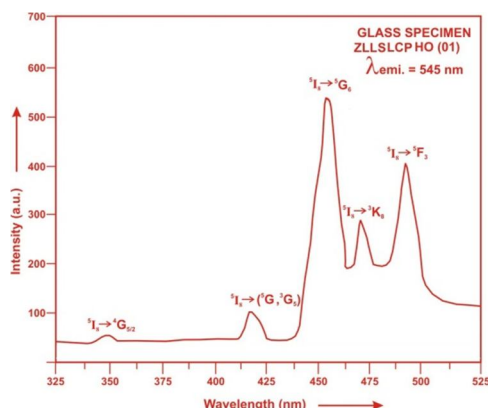


Fig. (4) Excitation spectrum of ZLLSLCP HO (01) glass.

E. Fluorescence Spectrum

The fluorescence spectrum of Ho^{3+} doped in zinc lithium lead sodalime cadmium phosphate glass is shown in Figure 5. There are eleven broad bands observed in the Fluorescence spectrum of Ho^{3+} doped zinc lithium lead sodalime cadmium phosphate glass. The wavelengths of these bands along with their assignments are given in Table 5. The peak with maximum emission intensity appears at 2035 nm and corresponds to the ($^5\text{I}_7 \rightarrow ^5\text{I}_8$) transition.

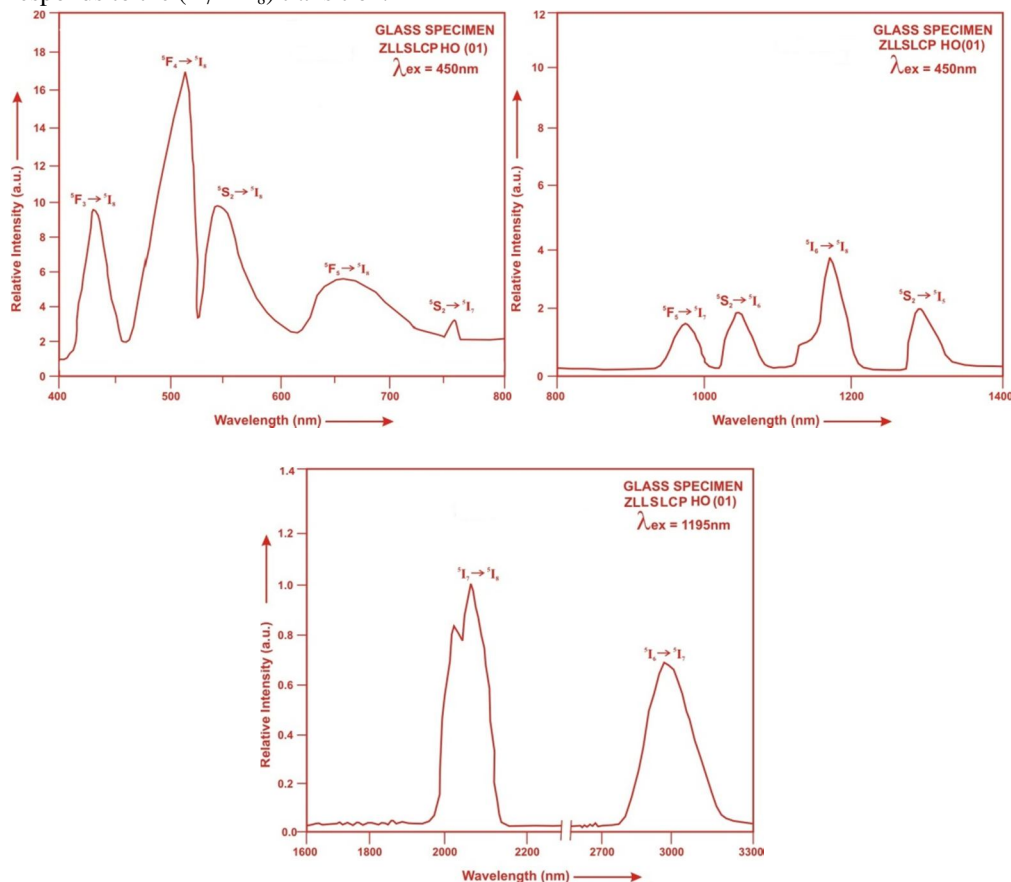


Fig. (5). Fluorescence spectrum of ZLLSLCP HO (01) glass.

Table5: Emission peak wave lengths (λ_p),radiative transition probability (A_{rad}),branching ratio (β),stimulated emission cross-section (σ_p) and radiative life time(τ_R) for various transitions in Ho^{3+} doped ZLLSLCP glasses.

| Transition | λ_{max} (nm) | ZLLSLCP (HO 01) | | | | ZLLSLCP (HO 1.5) | | | | ZLLSLCP (HO 02) | | | |
|-----------------------------------------|--------------------------------|---------------------------------|---------|-----------------------------------------------|-----------------------|---------------------------------|---------|-----------------------------------------------|-----------------------|---------------------------------|---------|-----------------------------------------------|---------------------------------------------|
| | | $A_{\text{rad}}(\text{s}^{-1})$ | β | σ_p (10^{-20} cm^2) | $\tau_R(\mu\text{s})$ | $A_{\text{rad}}(\text{s}^{-1})$ | β | σ_p (10^{-20} cm^2) | $\tau_R(\mu\text{s})$ | $A_{\text{rad}}(\text{s}^{-1})$ | β | σ_p (10^{-20} cm^2) | τ_R (10^{-20} cm^2) |
| $^5\text{F}_3 \rightarrow ^5\text{I}_8$ | 435 | 4421.05 | 0.2476 | 0.599 | 5601.28 | 4401.73 | 0.2480 | 0.585 | 5634.16 | 4366.81 | 0.2480 | 0.570 | 5680.07 |
| $^5\text{F}_4 \rightarrow ^5\text{I}_8$ | 501 | 7060.83 | 0.3955 | 1.237 | | 7017.17 | 0.3954 | 1.213 | | 6961.25 | 0.3954 | 1.187 | |
| $^5\text{S}_2 \rightarrow ^5\text{I}_8$ | 555 | 1846.68 | 0.1034 | 0.434 | | 1837.34 | 0.1035 | 0.427 | | 1822.76 | 0.1035 | 0.416 | |
| $^5\text{F}_5 \rightarrow ^5\text{I}_8$ | 652 | 2005.98 | 0.1124 | 0.729 | | 1990.59 | 0.1122 | 0.714 | | 1974.64 | 0.1122 | 0.698 | |
| $^5\text{S}_2 \rightarrow ^5\text{I}_7$ | 761 | 1406.48 | 0.0788 | 1.119 | | 1399.37 | 0.0788 | 1.100 | | 138.83 | 0.0789 | 1.073 | |
| $^5\text{F}_5 \rightarrow ^5\text{I}_7$ | 995 | 464.43 | 0.0260 | 1.194 | | 459.27 | 0.0259 | 1.166 | | 453.97 | 0.0258 | 1.131 | |
| $^5\text{I}_6 \rightarrow ^5\text{I}_8$ | 1032 | 214.79 | 0.0120 | 0.692 | | 213.54 | 0.0120 | 0.678 | | 211.84 | 0.0120 | 0.660 | |
| $^5\text{S}_2 \rightarrow ^5\text{I}_5$ | 1195 | 245.24 | 0.0138 | 1.212 | | 243.57 | 0.0137 | 1.189 | | 241.31 | 0.0137 | 1.164 | |
| $^5\text{S}_2 \rightarrow ^5\text{I}_6$ | 1310 | 65.44 | 0.0037 | 0.623 | | 65.08 | 0.0037 | 0.610 | | 64.58 | 0.0037 | 0.592 | |
| $^5\text{I}_7 \rightarrow ^5\text{I}_8$ | 2035 | 97.37 | 0.0055 | 4.653 | | 96.65 | 0.0054 | 4.557 | | 95.71 | 0.0054 | 4.453 | |
| $^5\text{I}_6 \rightarrow ^5\text{I}_7$ | 2925 | 24.78 | 0.0014 | 3.907 | | 24.55 | 0.0014 | 3.823 | | 24.27 | 0.0014 | 3.728 | |

V. CONCLUSION

In the present study, the glass samples of composition $(35x)\text{P}_2\text{O}_5:10\text{ZnO}:10\text{Li}_2\text{O}:10\text{PbO}:10\text{CaO}:10\text{Na}_2\text{O}:15\text{CdO}:x\text{Ho}_2\text{O}_3$, (where $x=1, 1.5$ and $2\text{mol } \%$) have been prepared by melt-quenching method. The value of stimulated emission cross-section (σ_p) is found to be maximum for the transition ($^5\text{I}_7 \rightarrow ^5\text{I}_8$) for glass ZLLSLCP (HO 01), suggesting that glass ZLLSLCP (HO 01) is better compared to the other two glass systems ZLLSLCP (HO1.5) and ZLLSLCP (HO 02). The large stimulated emission cross section in bismuth borate glasses suggests the possibility of utilizing these systems as laser materials.

REFERENCES

- [1] Alqarni, A. S., Hussin, R., Alamri, S.N., Ghoshal, S.K. (2020). Tailored structures and dielectric traits of holmium ion-doped zinc-sulpho-boro-phosphate glass ceramics. *Ceramics International*, 46(3):3282-3291
- [2] Nasser, K., Aseev, V., Ivanov, S., Ignatiev, A. and Nikonorov, N. (2019). Optical spectroscopic properties and Judd-ofelt analysis of Nd^{3+} doped photo thermo refractive glass. *J. lumen*. 213, 255-262.
- [3] Nayab Rasool, S.K., Rama Moorthy, L. and Jayasankar, C.K. (2013). Spectroscopic investigation of Sm^{3+} doped phosphate based glasses for reddish orange emission. *Optical Communication*, 3115, 156-165.
- [4] Gokce, M., Kocyigit, D. (2021). Spectroscopic investigations of Dy^{3+} doped borogermanate glasses for laser and WLED applications. *Opt. Mater.* 89, 568-575.
- [5] Karki, S., Kesavulu, C.R., Kim, H.J., Kaewkho, J., Chanthima, N., Kothan, S., Kaewjaeng, S. (2019). Physical, optical and luminescence properties of the Dy^{3+} doped barium borophosphate glasses. *J. Noncryst. Solids*, 521, 119483.
- [6] Kaur, R., Rakesh, R.B., Mhatre, S.G., Bhatia, V., Kumar, D., Singh, H., Singh, S.P. and Kumar, A. (2021). Physical, optical, structural and thermoluminescence behavior of borosilicate glasses doped with trivalent neodymium ions. *Opt. Mater.* 117, 1-13.
- [7] Shoaib, N., Chanthima, N., Rooh, G., Rajaramakrishna, R. and Kaewkhao, J. (2019). Physical and luminescence properties of rare earth doped phosphate glasses for solid state lighting applications. *Thai Int. Res.* 14, 20-26.
- [8] Kashif, I., Ratep, A. (2021). Judd-Ofelt and luminescence study of Dysprosium-doped lithium borosilicate glasses for lasers and w-LEDs. *Bol. Soc. Esp. Ceram. Vidr.* 61, 1-12.
- [9] Liu, L., Shi, Z., Song, Q., Li, D., Li, N., Xue, Y., Xu, J., Xu, J., Wang, X. (2020). Judd-Ofelt analysis and spectroscopic study of $\text{Tb}:\text{CaF}_2$ and $\text{Tb}/\text{Pr}:\text{CaF}_2$ co-doped single crystals. *Opt. Mater.* 108, 1-5.
- [10] Marzouk, M.A. and Elbatal, H.A. (2021). Investigation of photoluminescence and spectroscopic properties of Sm^{3+} doped heavy phosphate glasses before and after gamma irradiation. 70, 1-10.
- [11] Smith, C.E., Brow, R.K. (2014). The properties and structure of zinc magnesium phosphate glasses. *J. Non-Cryst. Solids*. 390, 51-58
- [12] Ehrt, D., Ebeling, P., Natura, U. (2000). UV Transmission and radiation induced defects in phosphate and fluoride-phosphate glasses. *J. Non-Cryst. Solids*, 263, 240-250.
- [13] Devi, R. and Jayasankar, C. K. (1995). Optical properties of Nd^{3+} ions in lithium borate glasses. *Materials chemistry and phys.* 42, 106-119.
- [14] Suresh, K., Jayasankar, C.K. (2019). Conversion of blue-green photon into NIR photons in $\text{Ho}^{3+}/\text{Yb}^{3+}$ co-doped zinc tellurite glasses. *J. Alloys-Compd.* 788, 1048-1055.
- [15] Mahamuda, Sk., Swapna, K., Packiyaraj, P., Rao, A.S. and Prakash, G.V. (2013). Visible red, NIR and Mid-IR emission studies of Ho^{3+} doped Zinc Alumino Bismuth Borate Glasses. *Opt. Mater.* 36, 362-371.
- [16] Meena, S.L. (2020). Spectral and Thermal Properties of Ho^{3+} Doped in Zinc Lithium Alumino Antimony Borophosphate Glasses. *Int. J. Scie. Dev. Res.* 5, 127-133.
- [17] Kowalska, K., Kuwik, M., Pisarska, J. and Pisarski, W.A. (2022). Near-IR Luminescence of Rare-Earth Ions (Er^{3+} , Pr^{3+} , Ho^{3+} , Tm^{3+}) in Titanate-Germanate Glasses under Excitation of Yb^{3+} . 15, 1-13.
- [18] Cai, M., Zhou, B., Wang, F., Tian, Y., Zhou, J., Xu, S., Zhang, J. (2015). Highly efficient mid-infrared 2 μm emission in $\text{Ho}^{3+}/\text{Yb}^{3+}$ -codoped germanate glass. *Opt. Mater. Express*. 5, 1431-1439.
- [19] Gorller-Walrand, C. and Binnemans, K. (1988). Spectral Intensities of f-f Transition. In: Gshneidner Jr., K.A. and Eyring, L., Eds., *Handbook on the Physics and Chemistry of Rare Earths*, Vol. 25, Chap. 167, North-Holland, Amsterdam, 101-264.
- [20] Sharma, Y.K., Surana, S.S.L. and Singh, R.K. (2009) Spectroscopic Investigations and Luminescence Spectra of Sm^{3+} Doped Soda Lime Silicate Glasses. *Journal of Rare Earths*, 27, 773-780.
- [21] Judd, B.R. (1962). Optical Absorption Intensities of Rare Earth Ions. *Physical Review*, 127, 750-761.
- [22] Ofelt, G.S. (1962). Intensities of Crystal Spectra of Rare Earth Ions. *The Journal of Chemical Physics*, 37, 511.
- [23] Sinha, S.P. (1983). Systematics and properties of lanthanides, Reidel, Dordrecht. 1-8.
- [24] Krupke, W.F. (1974). *IEEE J. Quantum Electron QE*, 10, 450



10.22214/IJRASET



45.98



IMPACT FACTOR:
7.129



IMPACT FACTOR:
7.429



INTERNATIONAL JOURNAL FOR RESEARCH

IN APPLIED SCIENCE & ENGINEERING TECHNOLOGY

Call : 08813907089  (24*7 Support on Whatsapp)